Novel Mesoporous Materials with a Uniform Distribution of Organic Groups and Inorganic Oxide in Their Frameworks

Shinji Inagaki,*,† Shiyou Guan,† Yoshiaki Fukushima,† Tetsu Ohsuna,‡ and Osamu Terasaki§

Contribution from Toyota Central R&D Laboratories, Inc., Nagakute, Aichi 480-1192, Japan, the Institute for Materials Research, Tohoku University, Sendai 980-8577, Japan, and the Department of Physics, Graduate School of Science and CREST, JST, Tohoku University, Sendai 980-8578, Japan

Received May 19, 1999

Abstract: Novel organic−inorganic hybrid mesoporous materials have been synthesized, in which organic and inorganic oxide moieties are distributed homogeneously at the molecular level in the framework, forming a covalently bonded network. They are highly ordered at the mesoscale, with two- and three-dimensional hexagonal symmetries and well-defined external morphologies. Nitrogen adsorption measurements show a uniform pore-size distribution with pore diameters of 31 and 27 Å, and high surface areas of 750 and 1170 m^2/g. The synthetic procedure to polymerize the organosilane monomer containing two trialkoxysilyl groups in the presence of surfactant can be applied to the synthesis of a variety of highly ordered organic−inorganic hybrid mesoporous materials.

Introduction

Since the discovery of ordered mesoporous silicates M41S[1] and FSM-16[2] in 1992−93, a variety of ordered mesoporous materials have been synthesized by a template method, using supramolecular assembly of surfactant molecules. These materials have a range of framework compositions, morphologies, and pore structures. The framework composition has been studied extensively, since that governs catalysis and adsorption properties. Mesoporous materials now include a variety of inorganic materials, e.g., non-Si transition-metal oxides with high thermal stability[3] and metallic platinum.[4] Recently, functionalization with organic groups of ordered inorganic mesoporous[5−11] and microporous materials[12,13] has attracted much attention because new catalytic and adsorption functions can be introduced onto the internal pore surfaces through the direct design of organic functional groups. These organic-functionalized mesoporous materials have a heterogeneous structure composed of an inorganic main framework with an organic layer grafted onto the framework. Generally, they exhibit poorer structural ordering than nonfunctionalized inorganic mesoporous materials, evidenced by less-distinct X-ray diffraction patterns. On the other hand, many kinds of amorphous inorganic oxides, containing organic groups in their framework, have been derived by the sol−gel polymerization method.[14,15] Although these amorphous materials have a homogeneous distribution of organic groups and inorganic oxide in the framework,[15] they have disordered structures and scattered pore-size distributions.

Here we report the syntheses of novel organic−inorganic hybrid mesoporous materials with a homogeneous distribution of organic fragments and inorganic oxide *within* the framework, rather than end-grafted, exhibiting a highly ordered structure of uniform pores, which are quite different from the conventional organic-functionalized ordered mesoporous materials and sol−gel-derived porous hybrid organic−inorganic materials.

Experimental Section

Starting Material. The hybrid mesoporous materials can be synthesized using organometallic compounds with two or more metal alkoxyl groups as a starting material. In this study, we selected the organosilane compound 1,2-bis(trimethoxysilyl)ethane (BTME) in which an ethane ($-CH_2CH_2-$) fragment is attached to two trimethoxysilyl groups [$Si(OCH_3)_3$] at both ends. This organosilane compound has been used for the synthesis of amorphous porous hybrid materials in previous work.[16] BTME was prepared by addition of 1,2-bis-

* To whom correspondence should be addressed. E-mail: inagaki@mosk.tytlabs.co.jp.

† Toyota Central R&D Laboratories, Inc.

‡ Institute for Materials Research, Tohoku University.

§ Department of Physics, Graduate School of Science and CREST, JST, Tohoku University.

(1) (a) Kresge, C. T.; Leonowicz, M. E.; Roth, W. J.; Vartuli, J. C.; Beck, J. S. *Nature* **1992**, *359*, 710−712. (b) Beck, J. S.; Vartuli, J. C.; Roth, W. J.; Leonowicz, M. E.; Kresge, C. T.; Schmitt, K. D.; Chu, C. T−W.; Olson, D. H.; Sheppard, E. W.; McCullen, S. B.; Higgins, J. B.; Schlenker, J. L. *J. Am. Chem. Soc.* **1992**, *114*, 10834−10843.

(2) (a) Inagaki, S.; Fukushima, Y.; Kuroda, K. *J. Chem. Soc., Chem. Commun.* **1993**, 680−682. (b) Inagaki, S.; Koiwai, A.; Suzuki, N.; Fukushima, Y.; Kuroda, K. *Bull. Chem. Soc. Jpn.* **1996**, *69*, 1449−1457.

(3) Yang, P.; Zhao, D.; Margolese, D. I.; Chmelka, B. F.; Stucky, G. D. *Nature* **1998**, *396*, 152−155.

(4) Attard, G. S.; Bartlett, P. N.; Coleman, N. R. B.; Elliott, J. M.; Owen, J. R.; Wang, J. H. *Science* **1997**, *278*, 838−840.

(5) Burkett, S. L.; Sims, S. D.; Mann, S. *Chem. Commun.* **1996**, 1367−1368.

(6) Macquarrie, D. J. *Chem. Commun.* **1996**, 1961−1962.

(7) Lim, M. H.; Blanford, C. F.; Stein, A. *J. Am. Chem. Soc.* **1997**, *119*, 4090−4091.

(8) Fowler, C. E.; Burkett, S. L.; Mann, S. *Chem. Commun.* **1997**, 1769−1770.

(9) Feng, X.; Fryxell, G. E.; Wang, L.-Q.; Kim, A. Y.; Liu, J.; Kemner, K. M. *Science* **1997**, *276*, 923−926.

(10) Rhijin, W. M. V.; Vos, D. E. D.; Sels, B. F.; Bossaert, W. D.; Jacobs, P. A. *Chem. Commun.* **1998**, 317−318.

(11) Lim, M. E.; Blanford, C. F.; Stein, A. *Chem. Mater.* **1998**, *10*, 467−470.

(12) Maeda, K.; Kiyozumi, Y.; Mizukami, F. *Angew. Chem., Int. Ed. Engl.* **1994**, *33*, 2335−2337.

(13) Jones, C. W.; Tsuji, K.; Davis, M. E. *Nature* **1998**, *393*, 52−54.

(14) Baney, R. H.; Itoh, M.; Sakakibara, A.; Suzuki, T. *Chem. Rev.* **1995**, *95*, 1409−1430.

(15) Loy, D. A.; Shea, K. J. *Chem. Rev.* **1995**, *95*, 1431−1442.

10.1021/ja9916658 CCC: $18.00
Published on Web 10/04/1999

(trichlorosilyl)ethane (Shin-etsu Chemical Co., Ltd., 50 g) dropwise to a mixture of 200 g of $NaOCH_3$ solution (28% methanol solution) and 102 g of anhydrous methanol at 0 °C under stirring. After removal of methanol, distillation under vacuum gave 38.3 g (84 mol %) of BTME with purity >95% by GC. The synthesized BTME was characterized by ^1H and ^{13}C NMR and GC/MS spectroscopy.

Synthesis. BTME was added to a mixture of octadecyltrimethylammonium chloride [ODTMA, $C_{18}H_{37}N(CH_3)_3Cl$], sodium hydroxide (NaOH), and water (H_2O) under vigorous stirring at 25 °C. A white precipitate appeared immediately after mixing when the molar ratio of BTME:ODTMA:NaOH:H_2O was 1:0.12:1:231. The suspension was stirred at 25 °C for 24 h. When the molar ratio was 1:0.57:2.36:353, no precipitate appeared during stirring at 25 °C. Heating this clear solution at 95 °C after stirring for 14 h at 25 °C brought about precipitation, and the suspension was kept at 95 °C for 21 h. The two kinds of precipitates were filtered and washed with deionized water. The precipitated powders were confirmed to be ordered mesostructures by X-ray powder diffraction (XRD) and transmission electron microscopy (TEM) experiments. The surfactant was removed by stirring 1.0 g of as-synthesized mesoporous materials in 150 mL of ethanol or water with 3.8 g of 36% HCl aqueous solution at 50 °C for 6 h. The filtered sample was washed twice with 150 mL of ethanol or water and dried. Elemental analysis and ^{13}C NMR spectra showed that the surfactants were removed completely by repeating this treatment twice. The synthetic yields of mesoporous materials were 43 and 35 mol % for the mixture ratios of 1:0.12:1:231 and 1:0.57:2.36:353, respectively.

Characterization. XRD patterns were obtained with a Rigaku RINT-2200 diffractometer using Cu Kα radiation. Scanning electron microscope (SEM) images were obtained on a JEOL JSM-890 field emission scanning microscope with an acceleration voltage of 10 kV for the two-dimensional (2D)-hexagonal sample and 3 kV for the three-dimensional (3D)-hexagonal sample. TEM images and electron diffraction (ED) patterns were recorded by JEM-4000EX with an acceleration voltage of 400 kV. The adsorption isotherms of nitrogen at the temperature of liquid nitrogen were measured using a Quantachrome Autosorb-1 system. The samples were outgassed for 2 h at room temperature before the measurements. The pore-size distributions were calculated using the Barrett−Joyner−Halenda (BJH) model from the adsorption branch isotherms. The ^{29}Si and ^{13}C NMR spectra were recorded on a Bruker MSL-300WB spectrometer at 59.62 MHz for ^{29}Si and 75.47 MHz for ^{13}C. Chemical shifts for both ^{29}Si and ^{13}C NMR were referenced to trimethylsilane (TMS) at 0 ppm.

Results and Discussion

The XRD patterns of the two mesoporous materials without surfactants are shown in Figure 1. One sample shows three clear diffraction peaks with lattice spacings of $d = 49.4$, 28.5, and 24.7 Å and three additional weak peaks with $d = 16.5$, 14.3, and 13.7 Å (Figure 1a). They can be indexed to a 2D-hexagonal lattice with lattice constant $a = 57.0$ Å as shown in Figure 1a. The material with one-dimensional channels arranged in a hexagonal net is defined as 2D-hexagonal since the diffraction pattern shows 2D *p*6*mm* symmetry. Although the 2D-hexagonal mesophase is of a typical symmetry observed in ordered inorganic mesoporous materials such as MCM-41[1] and FSM-16,[2] they usually show only four X-ray diffraction peaks of (10), (11), (20), and (21). The appearance of the (30), (22), and (31) reflections with large scattering angles indicates that the mesoporous material has a high degree of mesoscopic order.[17,18] Another sample shows several diffraction peaks with spacings of $d = 47.3$, 44.3, 42.0, 27.7, 25.6, and 23.6 Å that can be indexed to a 3D-hexagonal lattice with lattice constants $a = 88.6$ Å and $c = 55.4$ Å (Figure 1b). The unit cell parameter

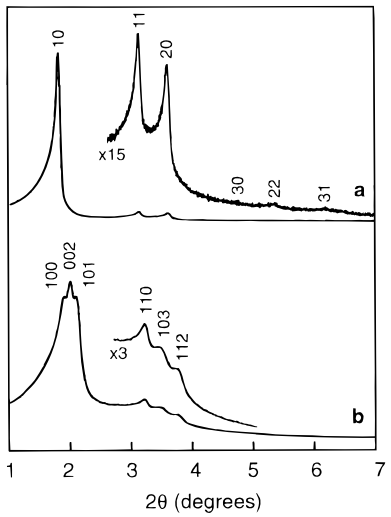

Figure 1. X-ray diffraction patterns of the mesoporous materials prepared from the reaction mixture in a molar ratio of (a) BTME:ODTMA:NaOH:H_2O = 1:0.57:2.36:353 and (b) BTME:ODTMA:NaOH:H_2O = 1:0.12:1:231. The peaks were indexed as 2D-hexagonal symmetry (a) and 3D-hexagonal symmetry (b).

ratio is $a/c = 1.60$, which is very close to the value of 1.633 for an ideal hexagonal close-packed (hcp) phase. Only two mesoporous silica materials with 3D-hexagonal symmetry have been reported previously, SBA-2[19] and SBA-12.[20] Our 3D-hexagonal mesoporous material also has higher structural ordering than SBA-2 and SBA-12 since the material shows a more distinct peak separation in the XRD pattern.[19,20]

Well-defined external morphologies of the materials are observed in the SEM images (Figure 2). In the 2D-hexagonal sample, rodlike particles with a hexagonal cross-section, a few micrometers in diameter and 10−20 μm in length, predominate (Figure 2a). The 3D-hexagonal sample shows spherical particles with diameters in the range of 0.1−10 μm (Figure 2b). The 2D- and 3D-hexagonal symmetries were confirmed by TEM. High-resolution (HR) TEM images of the 2D-hexagonal mesoporous sample show a clear hexagonal arrangement of pores with uniform size (Figure 3). No structural ordering in the pore wall was observed in the image. The corresponding ED pattern shows sharp reflections with hexagonal symmetry extending to the sixth order, suggesting excellent long-range order in the mesophase (Figure 3, inset). Comparison of the image (Figure 3) with images recorded from the as-synthesized 2D-hexagonal material shows that the framework structure is not affected by removal of the surfactant. We can also observe the channels running parallel to the rod from the same sample when electron incidence is perpendicular to the rod axis. These observations confirm that the pore structure consists of a hexagonal array of uniform 1D channels for the 2D-hexagonal sample, corresponding to the XRD result. The 3D-hexagonal mesophase was also confirmed by a series of ED patterns taken from the same particle with different directions of the incident electrons. However, we could recognize cubic/hexagonal intergrowth in some of the HRTEM images of the particles.

Nitrogen adsorption isotherms were measured for the 2D- and 3D-hexagonal mesoporous materials as shown in Figure 4. The BJH pore-size distributions were calculated from the isotherms (Figure 4, inset). The pore sizes are distributed over

(16) Oviatt, H. W.; Shea, K. J.; Small, J. H. *Chem. Mater.* **1993**, *5*, 943−950.

(17) Huo, Q.; Margolese, D. I.; Stucky, G. D. *Chem. Mater.* **1996**, *8*, 1147−1160.

(18) Zhao, D.; Feng, J.; Huo, Q.; Melosh, N.; Fredrickson, G. H.; Chmelka, B. F.; Stucky, G. D. *Science* **1998**, *279*, 548−552.

(19) Huo, Q.; Leon, R.; Petroff, P. M.; Stucky, G. D. *Science* **1995**, *268*, 1324−1327.

(20) Zhao, D.; Huo, Q.; Feng, J.; Chmelka, B. F.; Stucky, G. D. *J. Am. Chem. Soc.* **1998**, *120*, 6024−6036.

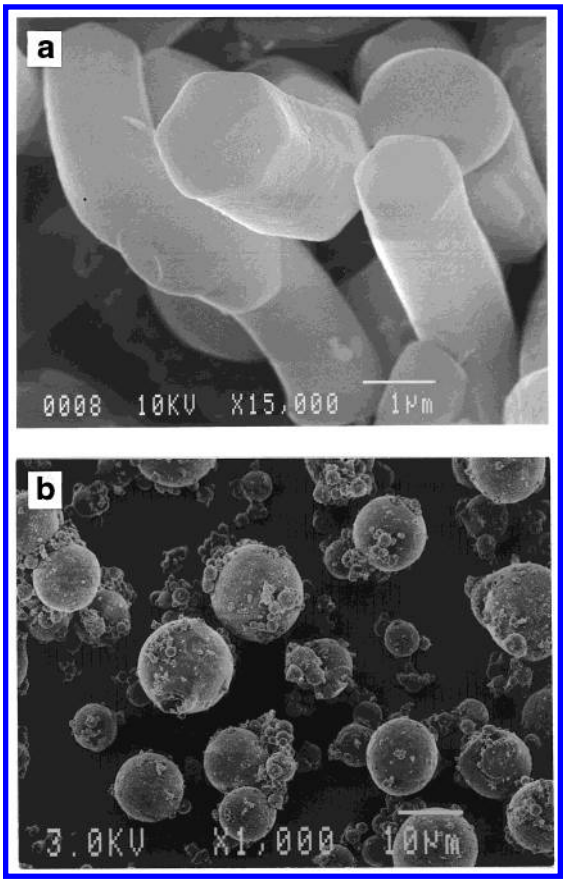

Figure 2. Scanning electron micrographs of the mesoporous materials with (a) 2D-hexagonal and (b) 3D-hexagonal symmetry.

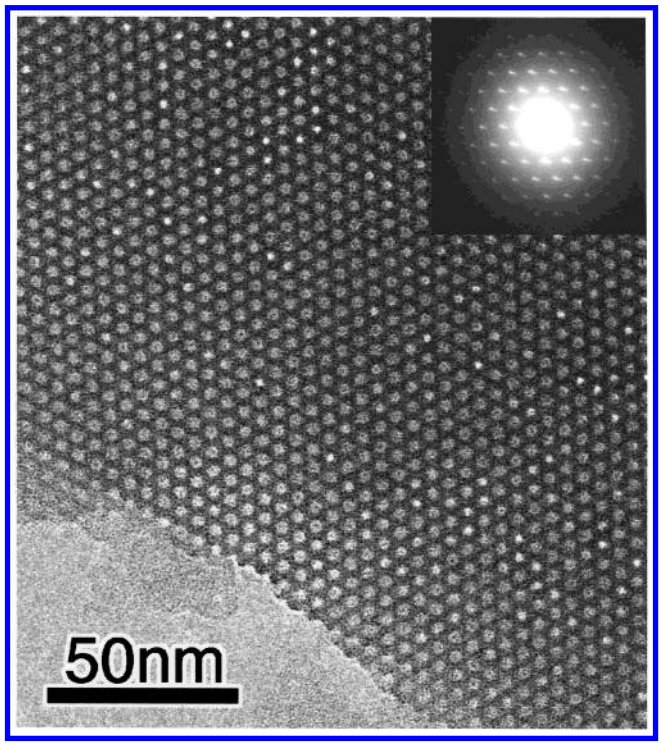

Figure 3. Transmission electron micrograph and electron diffraction pattern (inset) of the mesoporous material with 2D-hexagonal symmetry.

a very narrow range, centered on 31 and 27 Å for the 2D- and 3D-hexagonal mesoporous materials, which coincide with the pore dimensions estimated from the HRTEM images. Brunauer−Emmett−Teller (BET) surface areas calculated from the experimental data at relative pressures of 0.05−0.25[21] in the

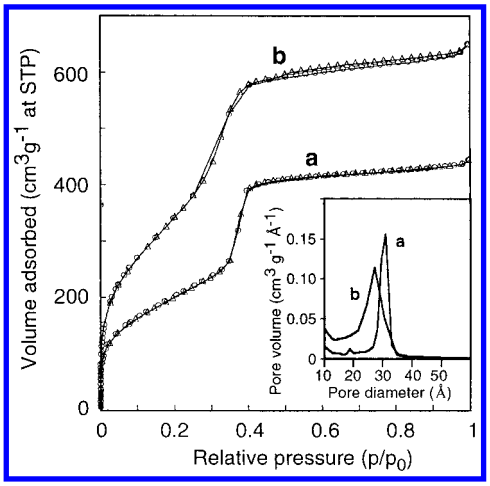

Figure 4. Nitrogen adsorption−desorption isotherms and pore-size distribution plot (inset) for the mesoporous materials with (a) 2D-hexagonal and (b) 3D-hexagonal symmetry.

isotherms are 750 and 1170 m^2 g^{-1} for the 2D- and 3D-hexagonal materials, which are also similar to those of inorganic mesoporous materials such as MCM-41 and FSM-16.

It was confirmed by magic angle spinning nuclear magnetic resonance (MAS NMR) experiments that the organic−inorganic moiety is the basic structural unit in the mesoporous materials. The ^{29}Si cross-polarization MAS NMR spectrum of the hybrid mesoporous material shows two signals at −57.0 and −66.0 ppm which are assigned to Si species covalently bonded to carbon atoms[8] [−57.0 ppm, $SiC(OH)(OSi)_2$; −66.0 ppm, $SiC(OSi)_3$, respectively] (Figure 5a). The ^{13}C cross-polarization (CP) NMR spectrum of the sample shows one signal at 5.4 ppm, which is assigned to an ethane fragment sandwiched by silicons ($Si-CH_2CH_2-Si$) and close to the chemical shift (2.0 ppm) of the BTME starting material (Figure 5b). The absence of SiO_4 species such as $Si(OH)(OSi)_3$ and $Si(OSi)_4$, whose signals are usually observed between −90 and −120 ppm,[8,9,13] confirms that carbon−silicon bond cleavage of the BTME starting organosilane compound has not occurred during the hydrolysis and polymerization (Figure 5c). No carbon signal due to ODTMA surfactant was observed in the ^{13}C NMR spectrum, and nitrogen was not detected in the elemental analysis, suggesting complete removal of the surfactant from the mesoporous materials by the solvent extraction process.

To our knowledge, these compounds are the first mesoporous materials whose frameworks have a completely uniform distribution of organic fragments incorporated within the inorganic oxide framework at the molecular level, and a periodic pore arrangement structure. In these hybrid mesoporous materials, the organic fragment is an essential component to construct the mesoporous wall, while the organic groups in conventional organic-functionalized mesoporous materials[5−11] are grafted onto the surface[7] of the inorganic wall. Thermal gravimetry analyses of the hybrid mesoporous materials show gentle weight loss due to the decomposition of ethane fragments at temperatures from 400 to 700 °C. The decomposition temperature is higher than that of ethyl groups grafted onto the framework surface of the conventional functionalized mesoporous material. The hybrid materials are also stable in boiling water. The XRD patterns of the hybrid mesoporous samples are essentially unchanged after treatment in boiling water for 8 h.

We can observe continuous lattices in HRTEM images throughout the rod-shaped and spherical particles, which indicate

(21) Gregg, S. J.; Sing, K. S. W. *Adsorption, surface area and porosity*; Academic: New York, 1982; pp 49−54.

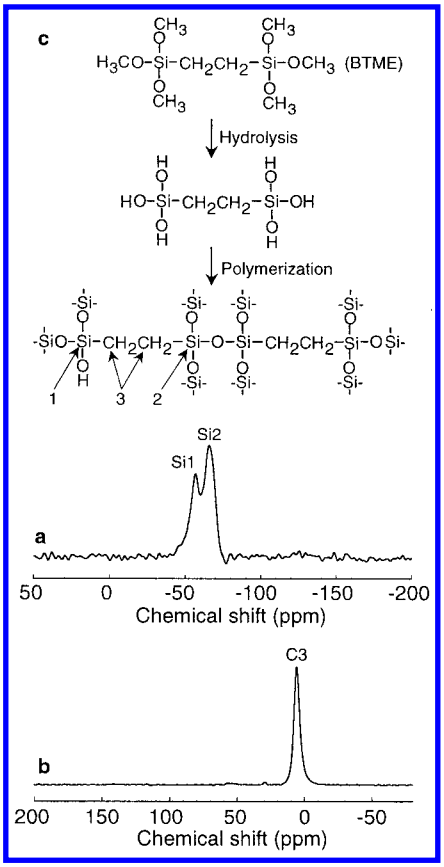

Figure 5. (a) ^{29}Si MAS NMR and (b) ^{13}C CP MAS NMR spectra of the mesoporous material with 2D-hexagonal symmetry. (c) Chemical reaction path for the formation of the organic−inorganic hybrid network structure with peak assignments of the NMR spectra.

that they are single crystals. Mesoporous silicas prepared from tetraethyl orthosilicate (TEOS) under acid conditions form a variety of characteristic shapes such as toroids, discoids, gyroids, etc. in micrometer sizes but rarely hexagonal rodlike shapes.[22] The formation of well-defined hexagonal rod shapes reflecting the 2D-hexagonal symmetry of pore arrangement in our hybrid mesoporous material suggests a low density of defects[22] in the material, which is supported by both the sharp ED patterns and regular pore arrangement in the HRTEM image with highly ordered symmetry. The organic-grafted mesoporous materials, which are synthesized from a mixture of organosilane with one silyl group [such as R−Si(OC$_2$H$_5$)$_3$, R is an organic group] and a silane such as TEOS usually have poor ordering, especially at a higher mixture ratio of organosilane/silane of over 0.25.[11] The formation of the highly ordered mesoporous material from 100% of the organosilane with two silyl groups as reported here is an exceptional case. The reason such a highly ordered structure is realized in the hybrid mesoporous materials remains uncertain, but we think that the flexible organic fragments in the framework relax the stress existing in the rigid inorganic silicate network. Rubber-like elasticity of the amorphous porous hybrid organic−inorganic material has been reported at high ratios of organic polymer to inorganic oxide,[15] which indicates that the incorporation of organic fragments in the main framework changes the mechanical properties of the material.

The formation of the 3D-hexagonal mesophase has not been previously observed in the alkyltrimethylammonium (ATMA) surfactant system including the lyotropic liquid crystal system and the ATMA/inorganic/water system. SBA-2 and SBA-12 with 3D-hexagonal symmetry have been synthesized from TEOS by using unusual surfactants with large hydrophilic headgroups such as divalent quaternary ammonium [C$_{18}$H$_{37}$N(CH$_3$)$_2$(CH$_2$)$_3$N-(CH$_3$)$_3$]Br$_2$[19] and nonionic alkyl poly(ethylene oxide) oligomer C$_{18}$H$_{37}$(OCH$_2$CH$_2$)$_{10}$OH,[20] which favor globular aggregates and the formation of the 3D-hexagonal mesophase.[19,20] In the BTME−ATMA system, the specific geometry of BTME with two silyl groups induces the formation of the unusual 3D-hexagonal mesophase. The anion charge density on organosilicate species formed by hydrolysis and oligomerization of BTME under a basic condition is lower than that on the silicate species formed from monosilane compounds, such as TEOS, because the silyl groups are separated by ethane fragments in the BTME derivative species. The low charge density enlarges the effective headgroup area of ATMA countercations in the BTME−ATMA assembly in accordance with the charge-density matching at the interface,[23] which induces the 3D-hexagonal mesophase. This result suggests that not only the geometry of the surfactant molecule[17] but also the geometry of the inorganic source can control the structure of the inorganic−surfactant mesophase.

This new approach to synthesis of the organic−inorganic hybrid mesoporous material has the potential to produce novel catalysts, adsorbents, and hosts for nanocluster synthesis. The conventional approach—grafting organic functional groups on the inorganic framework—has the advantage of introducing catalysis and adsorption properties of the organic functional groups directly, but the disadvantage of inactivation of catalytic sites on the inorganic framework through coverage with organic groups accompanying a decrease in the porosity. In our hybrid materials, both organic and inorganic active sites are exposed on the pore surface and the porosity is similar to that of nonmodified inorganic MCM-41 materials. Furthermore, novel active sites due to the hybridization of organic fragments and inorganic oxide on the molecular level can be designed in the uniform pores. We have also succeeded in synthesizing other ordered hybrid mesoporous materials containing methylene (−CH$_2$−), phenylene (−C$_6$H$_4$−), and vinylene (−CH═CH−) groups in their silicate networks. The properties of these materials can be manipulated by changing the organic fragments and inorganic compositions.

Conclusion

We have synthesized the first periodic mesoporous materials whose polymeric framework is composed of both inorganic and organic materials. The materials have a highly ordered structure with well-defined external morphologies reflecting the symmetries of the pore arrangement structure, whose ordering is higher than that of the conventional mesoporous materials. The synthesis procedure—to polymerize the organosilane monomer containing two or more alkoxysilyl groups in the presence of surfactant—can be applied to the synthesis of a variety of organic−inorganic hybrid mesoporous materials with a highly ordered structure.

Acknowledgment. We thank H. Kadoura (TCL, Japan) for SEM observations, N. Suzuki and Y. Seno (TCL, Japan) for discussion on TEM, and Stephen Hyde (ANU, Australia) for English correction. O.T. and T.O. thank CREST, Japan Science and Technology Corp. (JST), for support.

JA9916658

(22) Yang, H.; Coombs, N.; Ozin, G. A. *Nature* **1997**, *386*, 692−695.

(23) Firouzi, A.; Kumar, D.; Bull, L. M.; Besier, T.; Sieger, P.; Huo, Q.; Walker, S. A.; Zasadzinski, J. A.; Glinka, C.; Nicol, J.; Margolese, D.; Stucky, G. D.; Chmelka, B. F. *Science* **1995**, *267*, 1138−1143.